Supplementary information for the paper entitled

"June 2023 marine heatwave over the Northwest European shelf: origins, weather feedback and future recurrence."

by Berthou et al.

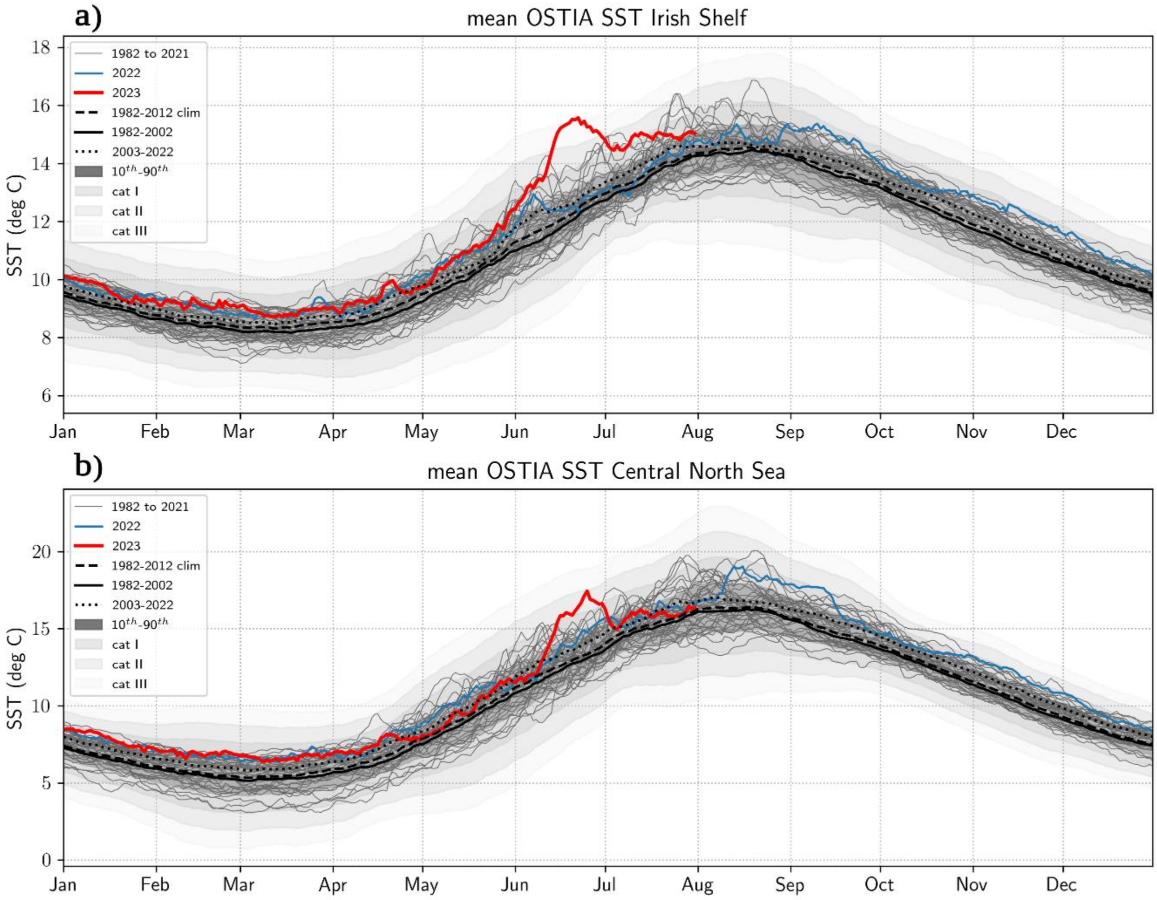

Figure S1: Same as Figure 1a but for the Irish shelf and Central North Sea regions highlighted in yellow and red in Fig. 1b.

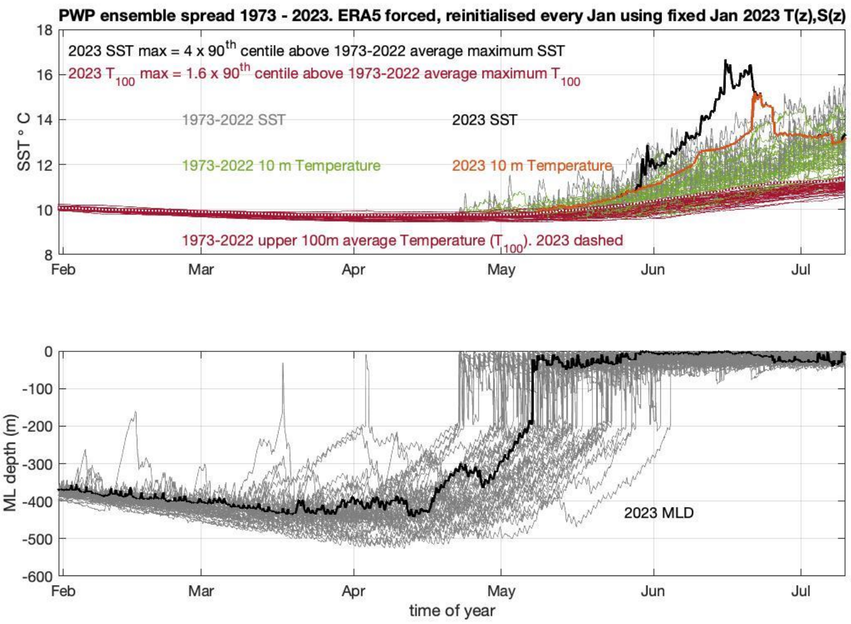

Figure S2: Sea surface temperature from a 1D ocean model (PWP) initialised on 11 Jan 2023 with an Argo temperature/salinity profile (closest to glider Eltanin in Fig. 2, in Rockall Trough) and forced with ERA5 hourly fluxes (SW, LW, Latent, Sensible, east and west turbulent stresses and Evaporation-Precipitation).

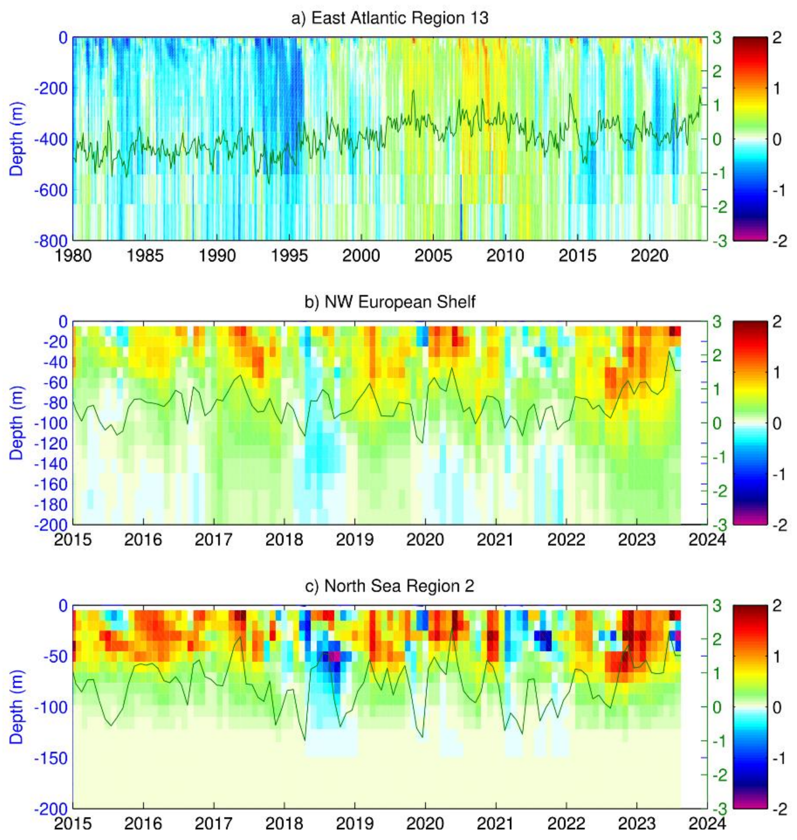

Figure S3: Anomalous EN4 potential temperature profiles a) East Atlantic region (region 13), b) NW European shelf (black region in Figure 1), c) Central North Sea (red region in Figure 1)

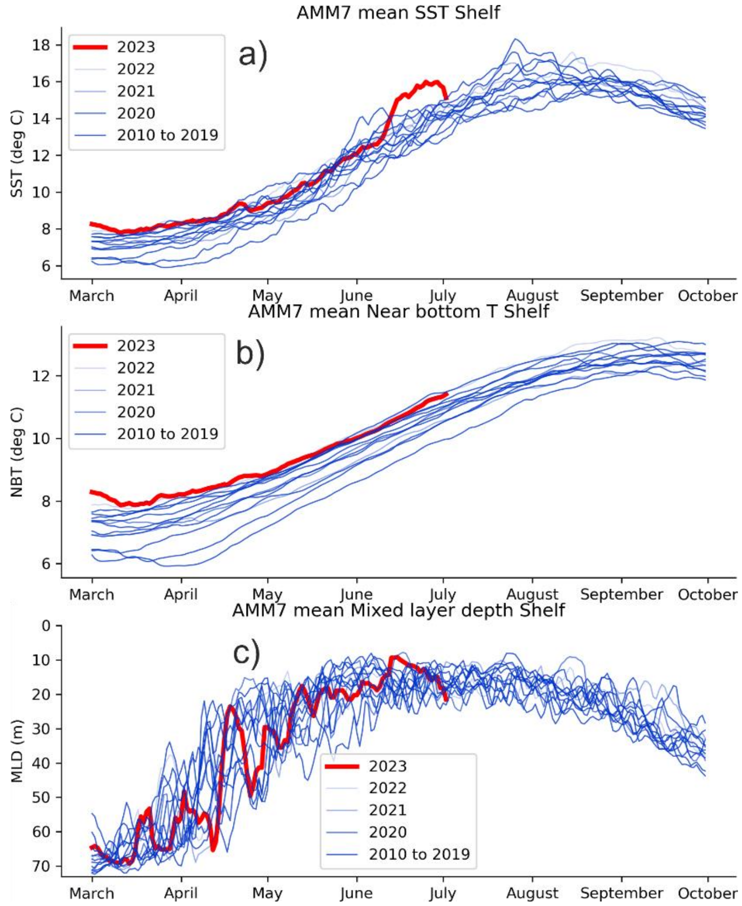

Figure S4: a) sea surface temperature, b) sea bottom temperature c) Surface Mixed layer depth for the OCN_amm7_RAN reanalysis

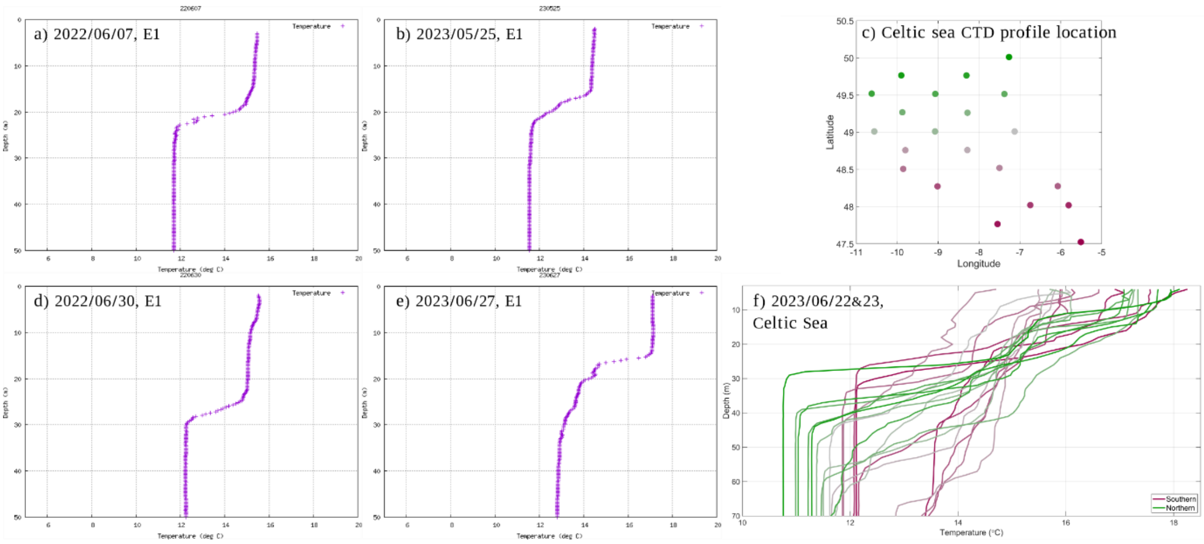

Figure S5: a, b, d, e: Potential temperature profiles at E1 (Western Channel Observatory, see location in Fig. 2) for different dates as noted on panel (note a&d for 2022, b&e for 2023). c, f: Potential temperature profiles in the Celtic sea, c shows the locations, f the profiles on 22&23/06/2023.

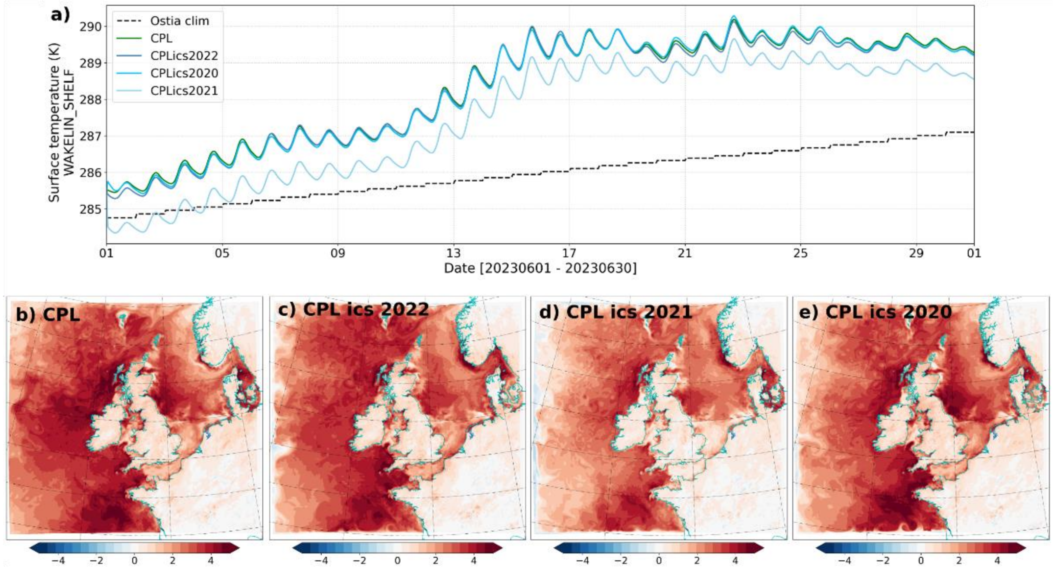

Figure S6: Coupled simulations, top: timeseries averaged over the shelf (NWS), bottom: 19-25th average anomaly (heatwave peak) in coupled simulations, with a 2023 restart and LBCs, or 2020, 2021 and 2022.

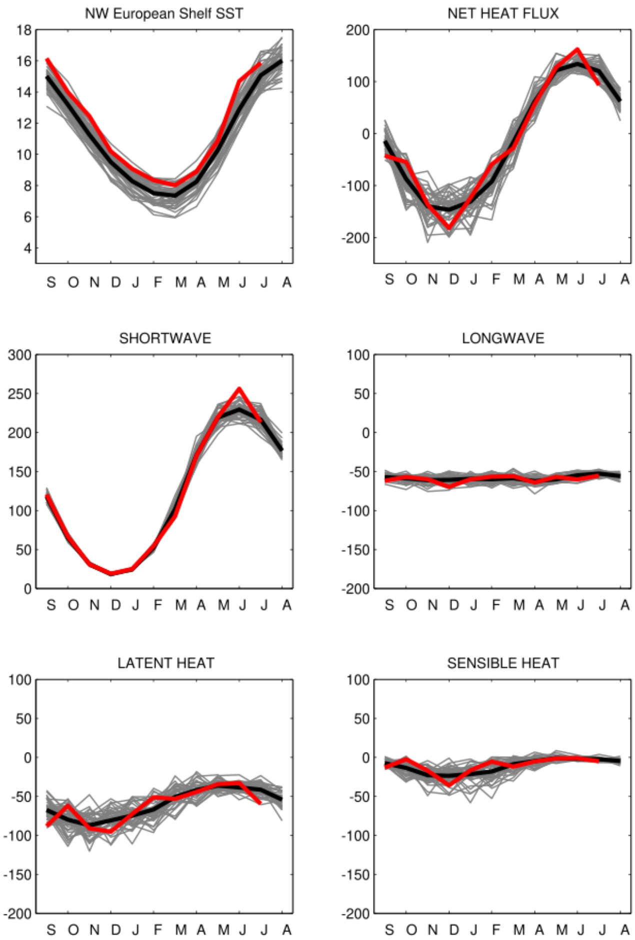

Figure S7: ERA5 monthly SST and atmospheric fluxes as stated on figure, averaged over the NWS, black is the mean for 1980-2023, each grey line is an individual year, red is 2023.

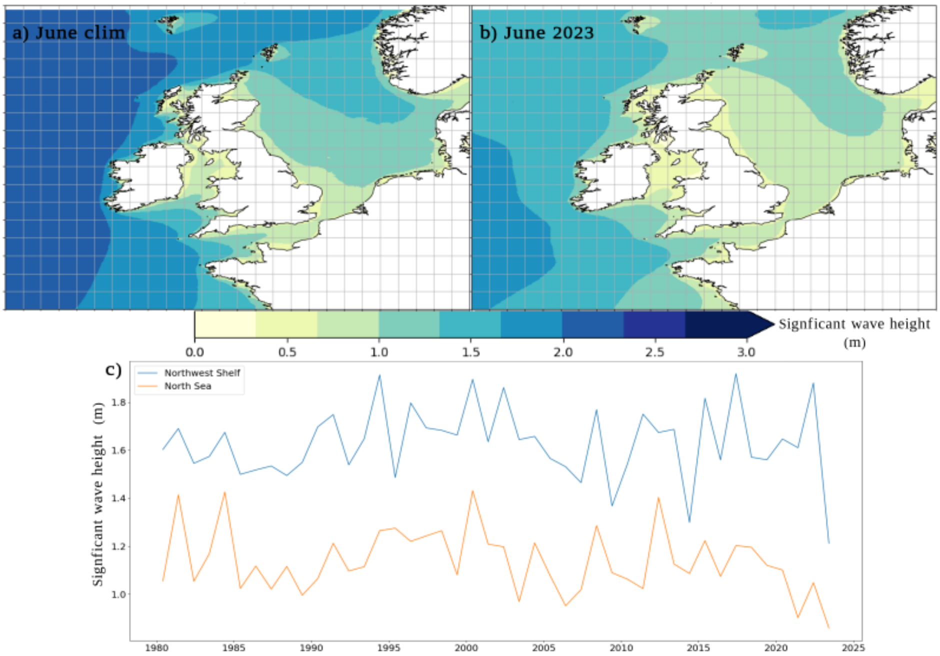

Figure S8: Average significant wave height calculated from the Copernicus Northwest shelf wave reanalysis (WAVamm15_RAN). Panels show a) spatial distribution for the period between 1980-2023 (June months only), b) is as a) but for June 2023, and c) time series of area average values between 1980-2023 (June months only) for the Northwest shelf (lon [–16, 10], lat [46, 63]) and North sea (lon [–2.6, 9], lat [51, 59]); note that June 2023 is the absolute minimum of the series.

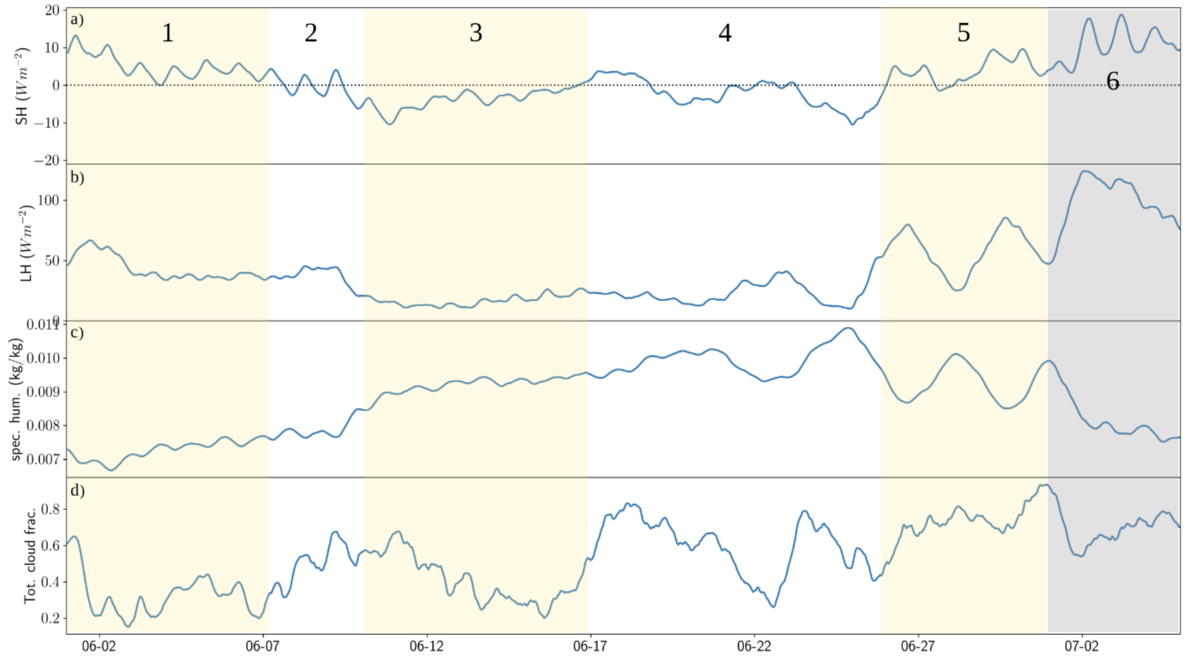

Figure S9: Same as Fig. 3 (average of ATMamm15 over the NWS) but a) with sensible heat flux (positive means heat lost by ocean), b) latent heat flux, c) specific humidity d) total cloud fraction (averaged over atmospheric depth).

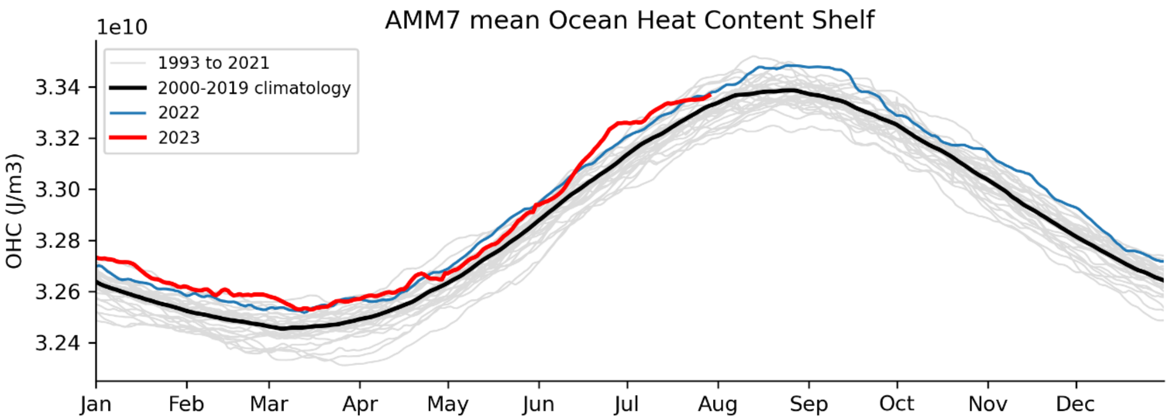

Figure S10: Ocean heat content averaged over the Northwest European shelf in the OCNamm7_reanalysis

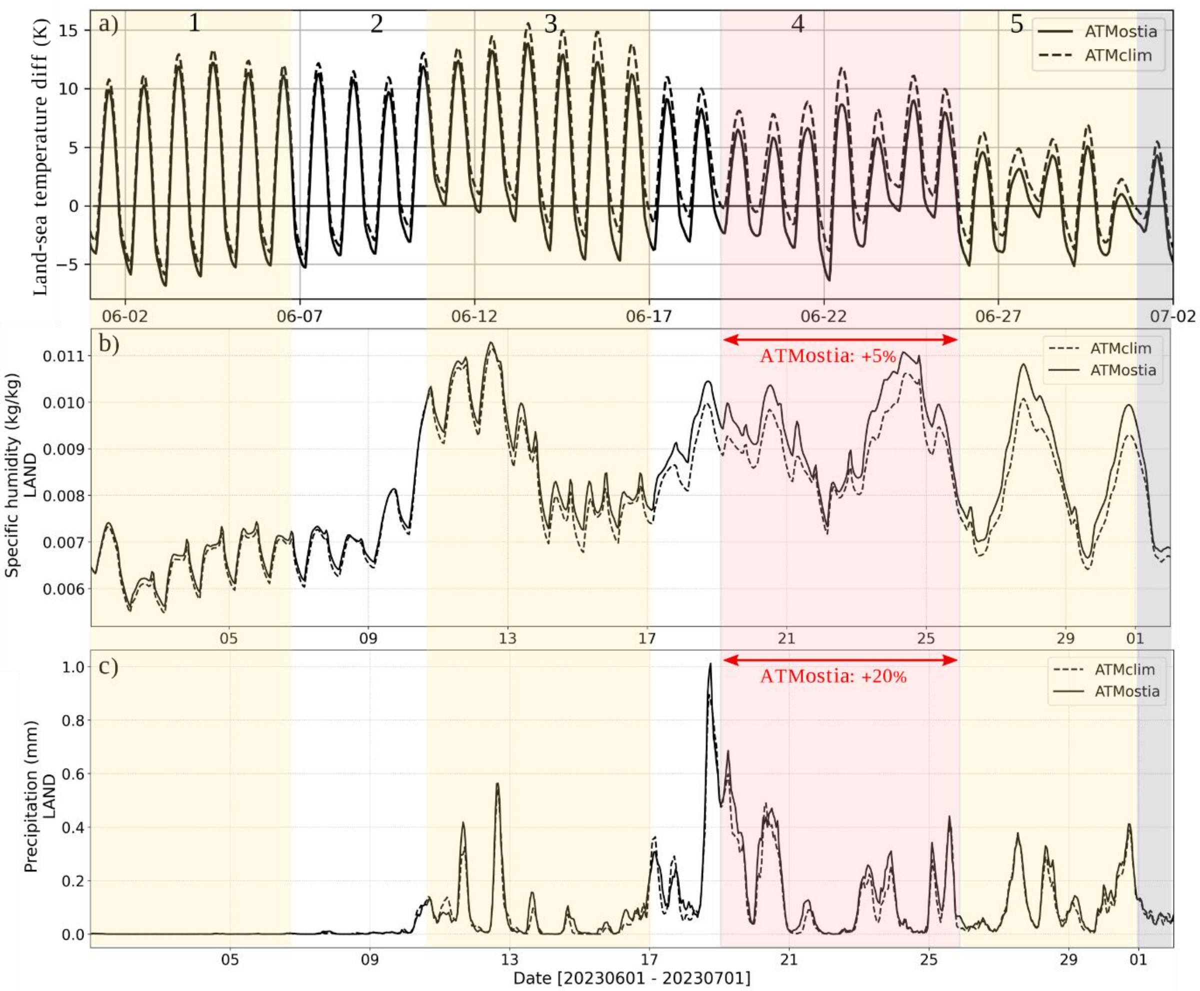

Figure S11: a) Land-sea temperature contrast calculated on a box centred around the British Isles () b) Specific humidity over the British Isles (land-only), ATMostia increase compared to ATMclim over June is 3.7%, and 5% for stage 4 (19th-25th), c) Hourly precipitation averaged over the British Isles (land-only), ATMostia increase compared to ATMclim over June is 13%, and 20% for stage 4 (19th – 25th).

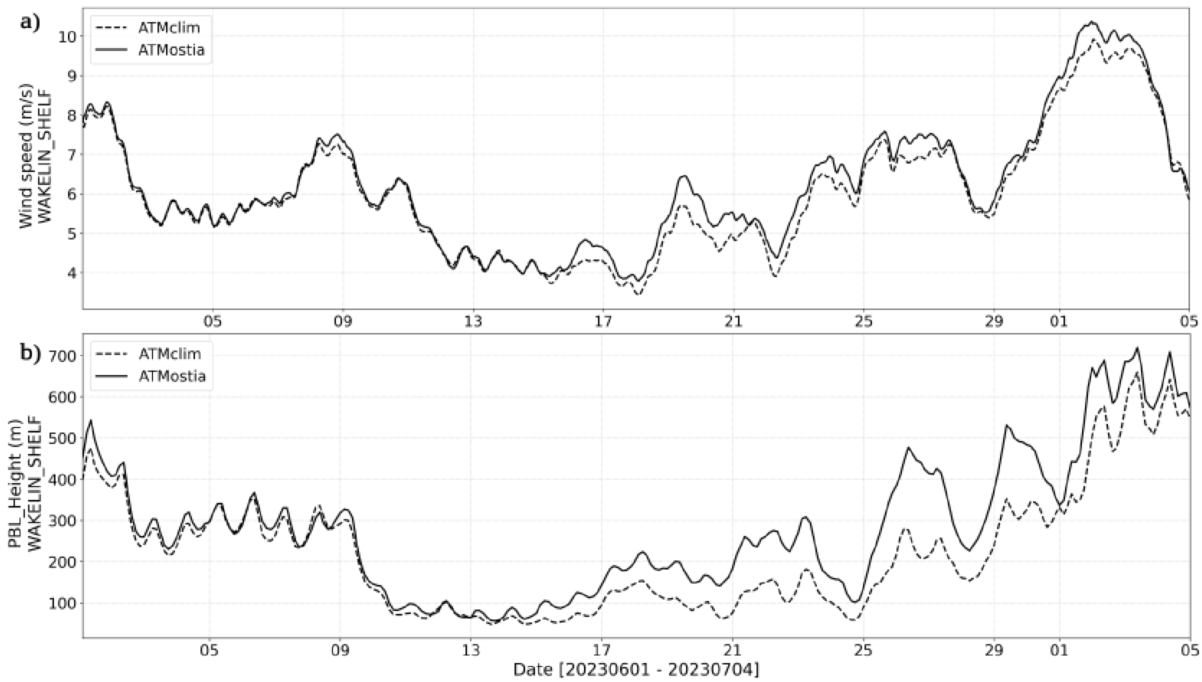

Figure S12: Average over the NWS of a) 10m wind speed (m/s) b) Planetary boundary layer height (m) for both ATMostia (with MHW) and ATMclim (no MHW).

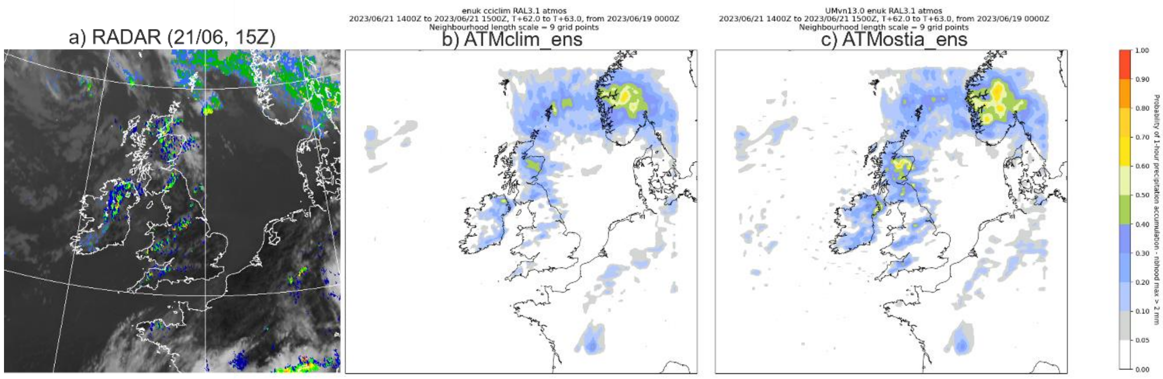

Figure S13: a) Precipitation on 21st of June at 15Z recorded by the RADAR network. b) Probability of precipitation >2mm/h in the ATMclim_ens (18-member ensemble forecast started on June 19th 00Z, without the MHW) and c) the ATMostia_ens (same ensemble but with the MHW).

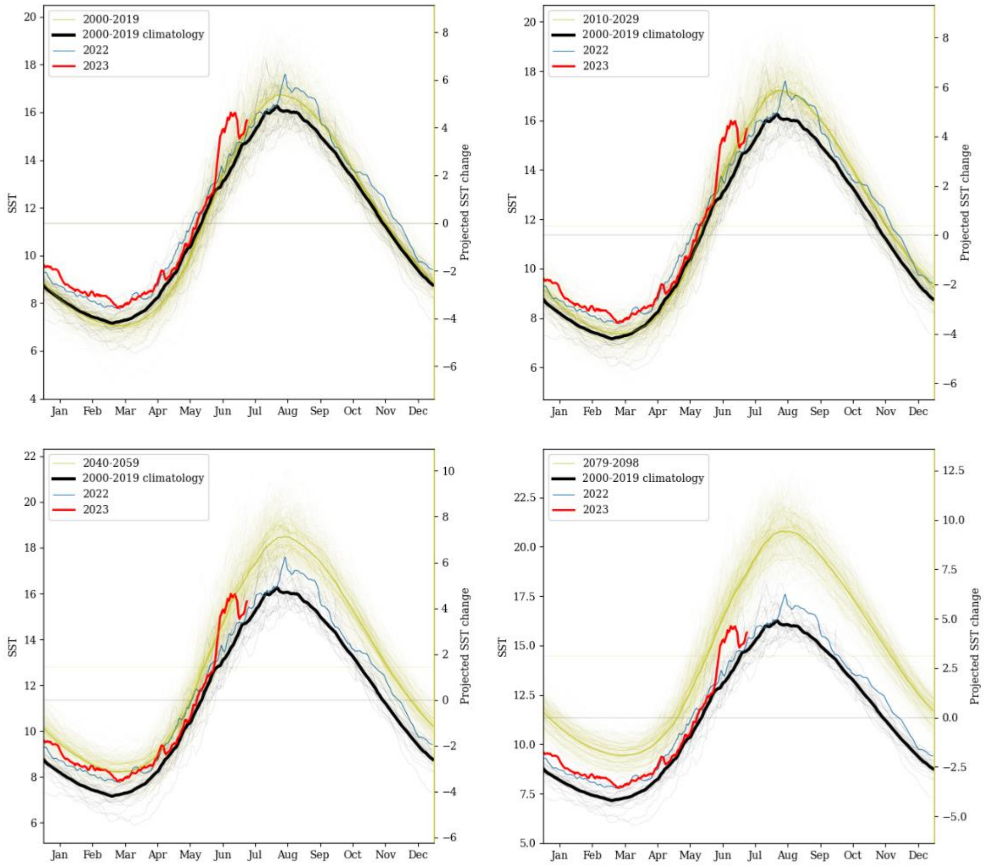

Fig S14 Projections of the NWS mean SST climatologies for four 20-year period, relative to the 2000-2019 baseline: a) 2000-2019, b) 2010-2029, c) 2040-2059, d) 2079-2098. Note Figure S13 is repeated from Figure 6d for ease of comparison. See Figure 6 for more details.

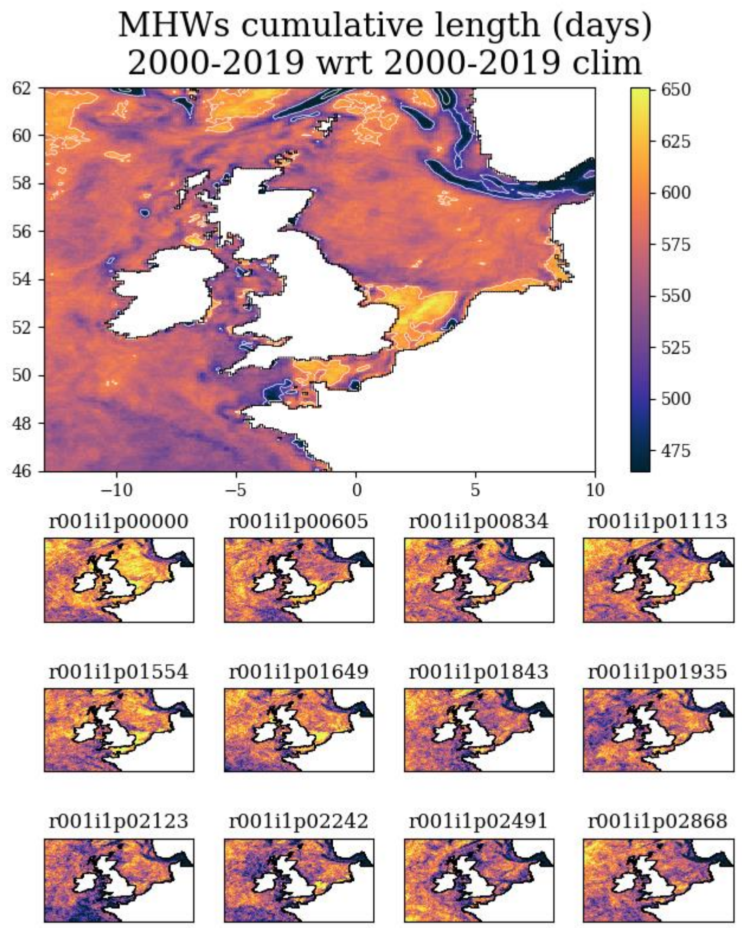

Fig S15 Total MHW duration (in days) per 20-year period (7200 days) for the period 2000-2019, relative to a threshold calculated from the 2000-2019 baseline. The main panel shows the ensemble mean based on the 12- ensemble member (in the lower panels) – All panels share the colour-bar and limits. The white contours in the upper panel match the ticks on the colour-bar.

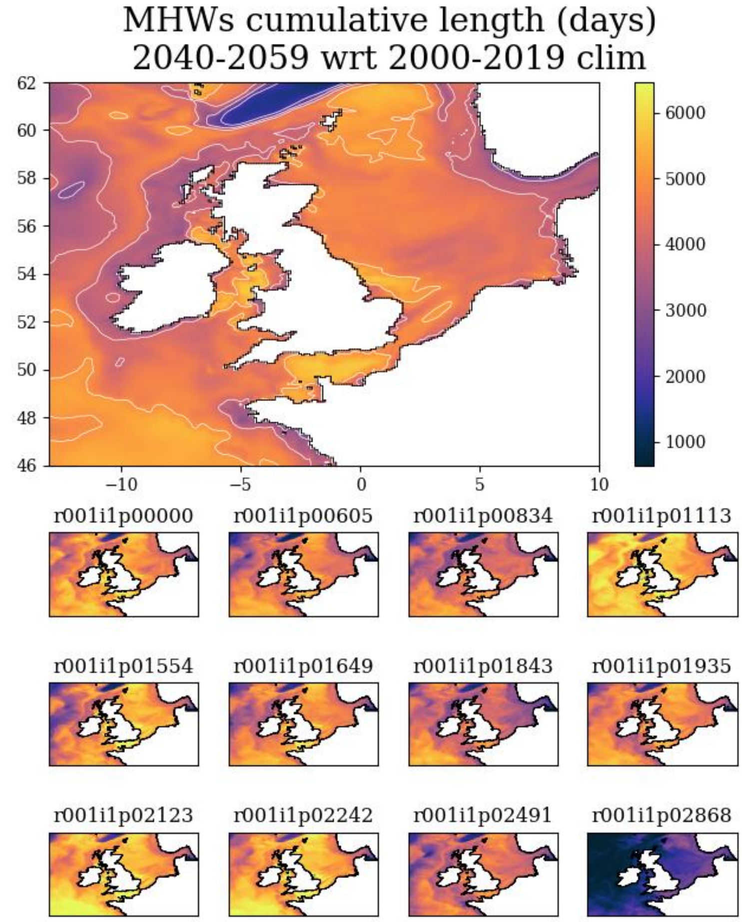

Fig S16 As Fig S15, but for the 2040-2059 period. See Fig S14 for details. Note the colour scale has changed from S14.

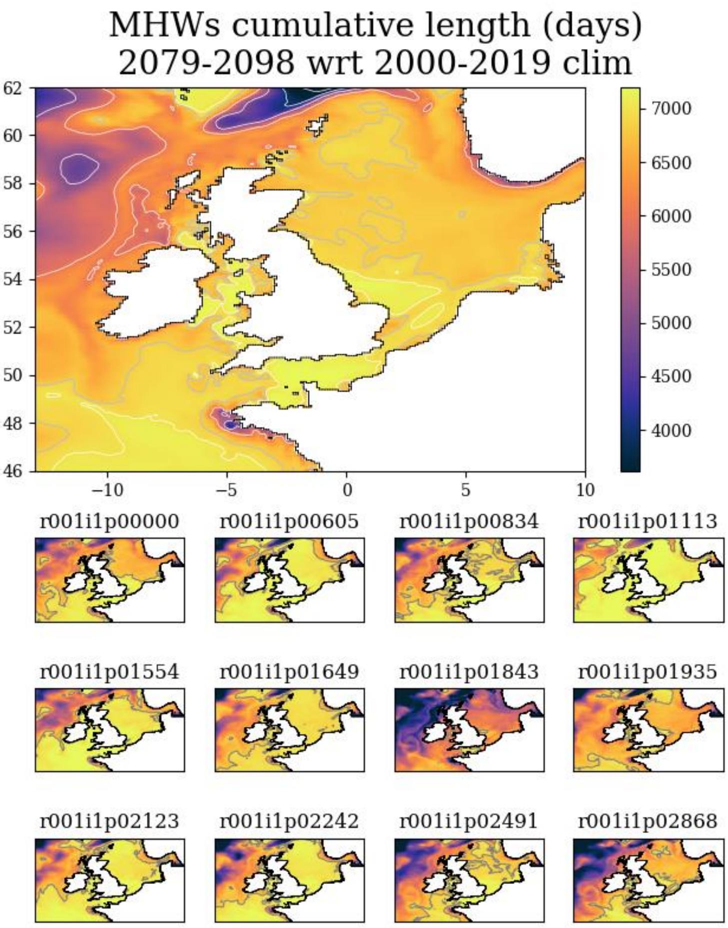

Fig S17 As Fig S14, but for the 2079-2098 period. See Fig S14 for details. The grey contour (not visible in previous plots) is for 6840 days – showing the grid-boxes that experience MHWs for more than 95% of the 20 year period. Note the colour scale has changed from S14.

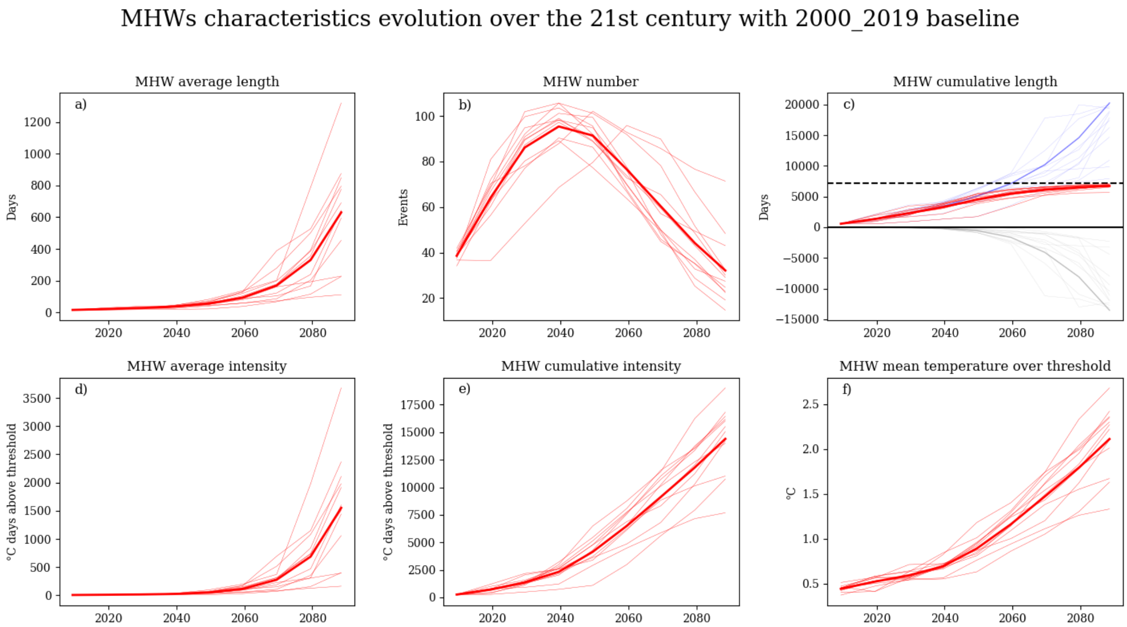

Figure S18 MHW statistics averaged over the NWS (using the Wakelin et al. 2012 NWS region) as calculated from overlapping 20-year periods. The ensemble mean is given (in bold), with the 12 ensemble members (in thinner lines). a) the *average MHW length; b) number of MHWs within the 20-year period; c) the total length of MHWs within the 20-year period , as calculated from the MHW algorithm(red), and (blue) derived as the product of Figure S17a and Figure S17b. The difference between the red and blue line, is their covariance (grey); d) the average intensity of the MHWs; e) the cumulative MHW intensity; and the derived average MHW temperature above the threshold. See text for details. Ensemble mean values are given in Table S1.*

Supplementary methodology

Climate analysis methodology

We use the latest set of marine climate projections for the NWS to assess how MHWs will be affected by climate change. These were developed by the Met Office as an extension of the latest UK marine climate projections UKCP18 (Murphy et al., 2018, Palmer et al. 2018). For UKCP18 a Perturbed Parameter Ensemble (PPE; Yamazaki et al., 2021) was run using the global climate model HadGEM3-GC3.05 (Williams et al., 2018; Yamazaki et al., 2021), under the RCP8.5 scenario. Twelve members of this PPE were downscaled with a shelf seas model configuration based on NEMO 4.0.4 (O'Dea et al., 2017; hereinafter CO9), as transient simulations (1980-2098). CO9 is a baroclinic tidal model, run on the 7km AMM7 domain, with 50-terrean following s-coordinate. As HadGEM3 GC3.05 was run on a 360-day calendar, CO9 was too this complicated the direct use of the Hobday MHW python tool box.

NWSPPE Monthly mean fields for all years and ensemble member are freely available (Tinker, 2023), but we have used their daily mean SST fields.

We first analysed the regional mean SST time series, using the Northern North Sea region (Wakelin et al., 2012) and the North West Shelf region (Tinker et al., 2019). We compared the NWSPPE SST climatology for the early (2000-2019), mid (2040-2059) and late century (2079-2098), and near-present day (2010-2029), but computing the 20-year climatological means, for each ensemble member, for each period, and then subtracted the early century annual mean value from each ensemble member to give an anomaly. This was plotted with the OCN_amm7_RAN time series in figure 6d and figure S14.

We developed a 2-dimensional implementation of the Hobday MHW method to give spatial summary statistics of the number of events, their average and total duration, and their average and total intensity (above a threshold) within a dataset. As we wanted to apply the method to both the climate data and the reanalysis, we implemented it for both the 360-day calendar and the Gregorian Calendar – the original Hobday method did not natively work for 360-day calendars). We included the minimum 5-day duration test of the Hobday MHW method (their option `minDuration=5`), but do not join two MHWs together that are separated by less than 2 days (their option: `joinAcrossGaps=False`, `maxGap=2`). This algorithm was evaluated against 30 time-series from points distributed across the domain, for all 12-ensemble member, giving 360 timeseries to give confidence that our methodology was replicating the Hobday Method (Figure S19). We also applied it to the reanalysis, to give confidence that the NWSPPE was able to give representation of reality.

We first created a climatology using the Hobday method. For a given 20-year period (2000-2019) we cycled through days of the year, taking the previous and subsequent 5 days, for all 20 years, giving 210 days of data. The mean and 90th percentile were then recorded to give the climatology and the threshold levels. These were then smoothed with a 31-day running mean. This was calculated for each ensemble member, and for the RAN.

We ran the MHW algorithm on each ensemble member separately. We cycled through the days of a 20-year period (e.g. 2000-2019, 2040-2059, 2079-2098 etc). For each day we loaded the

SST for that day from the ensemble member, and the climatological mean and threshold, and asked which grid boxes exceeded the threshold. We had a series of count, sum and sum of squares arrays to increment the duration, intensity (temperature above the threshold) and number of MHWs. We had a pair of map arrays for the current and previous days to record whether the grid box had a MHW or not. By comparing these Boolean arrays, we could ask if a grid box had a MHW starting (so the grid box was False for the previous day, and True for the current day – F-T), a MHW finishing (T-F), a MHW continuing (T-T) or no MHW (F-F). We then incremented a series of count and sum arrays for T-T, and F-T, and reset them for T-F. If the array counting the duration of the current MHW exceeded a duration threshold (5 days) we incremented the running total (sum and count) before resetting the current event counters. At the end of the run, the sum, sum or squares and count arrays were converted into mean and standard deviation, and recorded as NetCDF files for further analysis and visualisation.

To compare to the Hobday python toolbox, we extracted SST time series for 30 locations around the NWS (linearly interpolated from 360 days to 365.25 days) for all 12 ensemble members. These were analysed with the Hobday python toolbox, and the timings and characteristics of the individual events was compared. The time series averaged and cumulated statistics were also compared. When comparing all 360 time series, we find excellent agreement for the cumulative intensity, and cumulative intensity over the threshold ($r \approx 1.00$, ratio ≈ 0.98), and good agreement for the number of events ($r=0.93$, $m = 0.93$), and cumulative duration ($r=0.91$, $m \approx 1.00$). There is a slight offset in the cumulative duration, perhaps reflecting the `joinAcrossGaps` option that was not implemented in the 2d method.

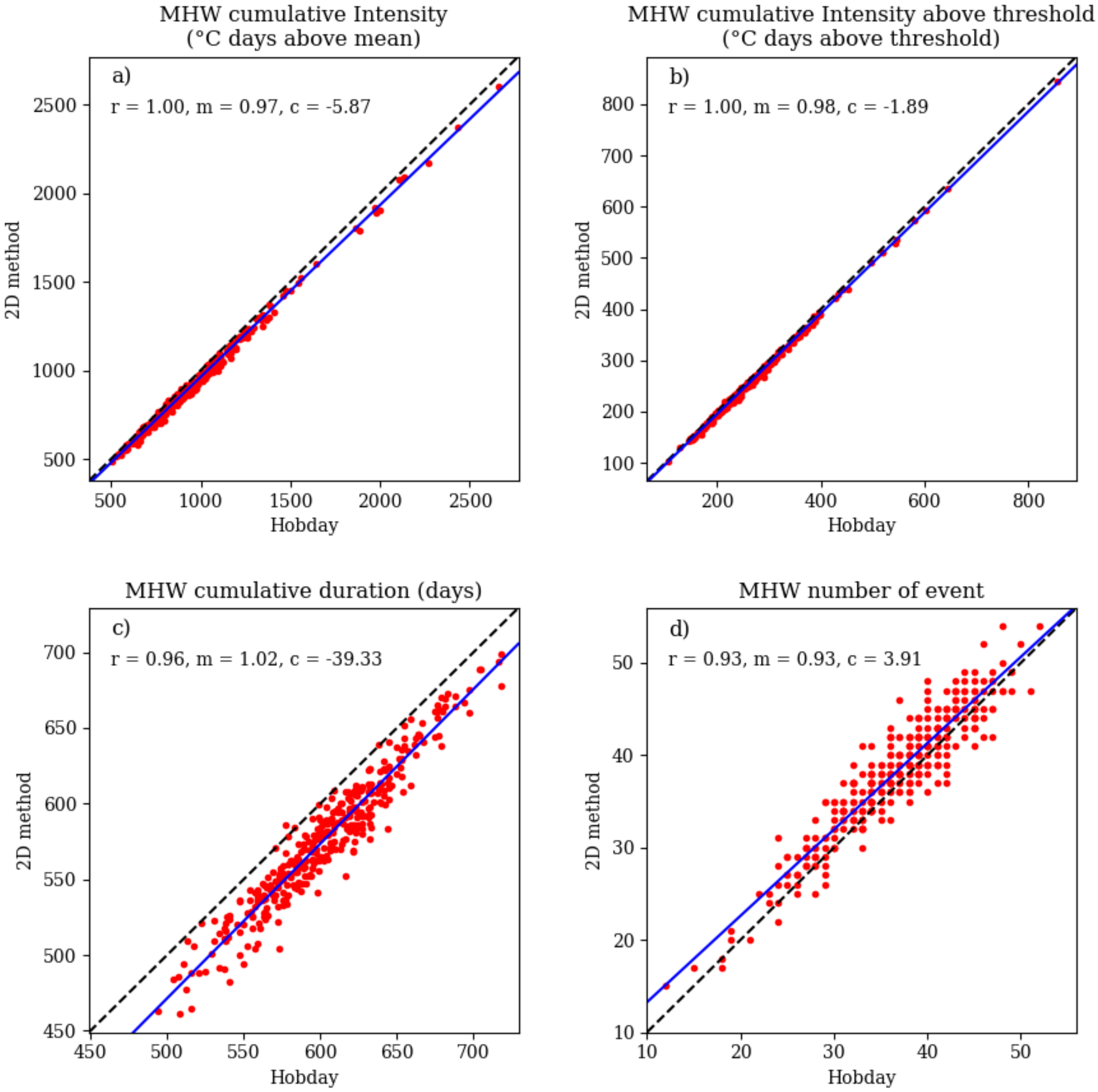

Figure S18 Comparison of the Hobday MHW method, and our two-dimensional implementation, based on 360 timeseries (30 random locations over all 12 ensemble members), for a) cumulative intensity above mean; b) cumulative intensity above the threshold; c) cumulative duration and d) number of events. Cumulative intensity above mean is not used in this study, but is an output from the Hobday MHW method, and so was assessed.

To assess how the NWSPPE simulated MHWs, we applied our MHWs algorithm to the daily mean SST from the RAN between 2000 - 2019, and compared them to the NWSPPE ensemble distribution and ensemble mean. We used the same methodology to calculate the climatology, with the additional step of averaging 28 February and 1 March to give values for 29February. We then compared the RAN MHW statistics to those of the ensemble mean, and asked whether the differences were less than the ensemble standard deviation. For all statistics considered (average length, number, cumulative length, average intensity, cumulative intensity), the RAN was within the ensemble spread, and generally close to the ensemble mean (Figure S20, Figure S21), so we considered our methodology and the NWSPPE fit-for-purpose.

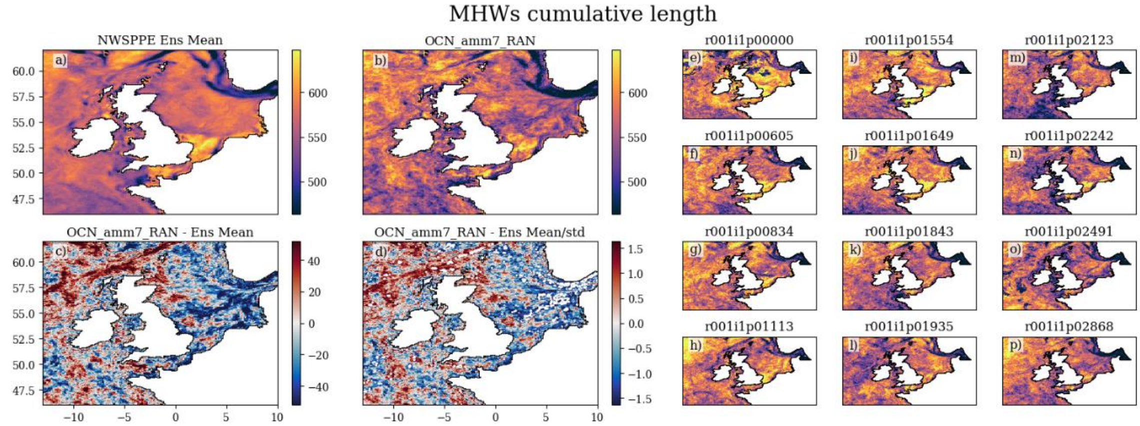

Figure S19 Comparison of the MHW cumulative length from the Hobday MHW analysis of the NWSPPE (OCN_amm7_proj) and OCN_amm7_RAN for the 2000 - 2019 period. MHW cumulative length is the total number of days (for a given grid box) under which a MHW is declared during the 20-year period. A) the NWSPPE ensemble mean; b) OCN_amm7_RAN; c) the difference between the OCN_amm7_RAN and the Ens Mean (positive values where OCN_amm7_RAN is greater than NWSPPE);d) the difference normalised by the NWSPPE ensemble spread – effectively the number of NWSPPE ensemble standard deviations the OCN_amm7_RAN is from the NWSPPE ensemble mean e-p) individual ensemble members.

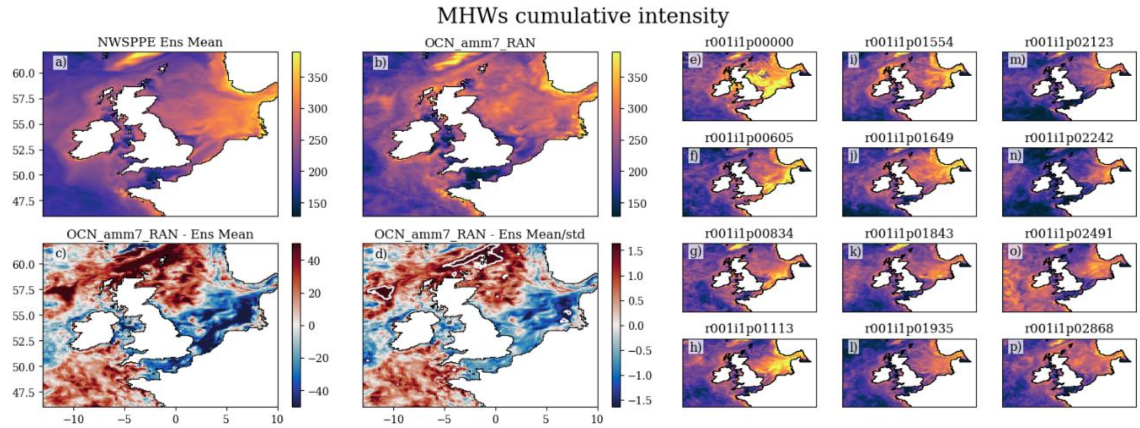

Figure S20 Comparison of the MHW cumulative intensity from the Hobday MHW analysis of the NWSPPE (OCN_amm7_proj) and OCN_amm7_RAN. MHW cumulative intensity is the total degree days above the 90th centile in the 20-year record. See figure S19 for details.

We then ran our MHW algorithm for each ensemble member, for overlapping 20-year periods (including 2000 - 2019, 2010 - 2029, 2020 - 2039, 2030 - 2049, 2040 - 2059, 2050 - 2069, 2060 - 2079, 2070 - 2089, 2079 - 2098) to show how the MHW characteristics change over the 21st century (Table S1). Figure S18 gives time series of the main MHW statistics averaged over the NWS (using the Wakelin et al. 2012 NWS region).

Given the main criteria for a MHW is that the temperature is greater than the 90th centile, and this period corresponds to the baseline period (from which the threshold is calculated), we could expect ~10% of days to have a MHW in the 2000 - 2019 baseline period (Figure S15, S20, Figure S18c), which corresponds to ~720 days for a 20-year period. The actual number (~568, Table S1) is lower given the secondary criterion that MHWs must be greater than 5 days.

We also expect the product of the average number of MHW and the average length of the MHWs (the blue lines in Figure S18c) to equal the cumulative length, which is what we see when looking at maps of these properties. When looking at regional mean time series (such as figure S18) this relationship holds for the early part of the time series, but starts to break down at about 2050, when, on average (across the NWS and Ensemble), the NWS experiences ~4000 days of MHW per 20-year period. This is because the product of two (regional) means is not the (regional) mean of the product – the difference is the covariance (the grey line in Figure S18c). As the climate warms, the number and length of the MHWs tend to covary, as some places tend to increase the number of MHWs, and others increase their duration, perhaps related to local variability.

The MHW intensity divided by the MHW length approximately gives the average temperature of the MHW over the threshold (based on the 2000 - 2019 90th centile). Figure S18f suggests the average MHWs temperature above the threshold increases from ~+0.5 °C to ~+2 °C.

Table S1 Ensemble and regional mean MHW statistics for the NWS region. These values are calculated from overlapping 20-year periods, and so represent the number/duration/intensity of MHWs for the 20-year period, which is 7200 days, given the 360 day calendar. These values are used in Figure S17.

Period	Central Year	Mean MHW duration	Number of MHWs	Total MHW duration (days)	% time as MHW	Mean MHW Intensity (°C days)	Total MHW Intensity (°C days)	Mean MHW Temperature above MHW threshold. (°C)	Covariance between MHW number and duration (days)	% of NWS grid-boxes with ensemble mean MHW duration >95% (6840/7200
2000-2019	**2009.5**	**15.28**	**38.59**	**567.91**	**7.89**	**6.77**	**251.28**	**0.44**	**-21.76**	**0**
2010-2029	2019.5	21.13	64.18	1341.81	18.64	11.03	704.35	0.52	-14.04	**0**
2020-2039	2029.5	27.06	86.12	2285.82	31.75	15.99	1351.12	0.59	-44.76	**0**
2030-2049	2039.5	36.05	95.36	3283.19	45.6	25.44	2316.85	0.69	-154.75	**0**
2040-2059	**2049.5**	**55.35**	**91.38**	**4502.48**	**62.53**	**51.74**	**4138.31**	**0.89**	**-555.84**	**0**
2050-2069	2059.5	92.89	76.54	5465.94	75.92	114.83	6486.89	1.16	-1643.2	**0**
2060-2079	2069.5	169.31	60.33	6109.05	84.85	276.67	9118.53	1.47	-4104.87	2.41
2070-2089	2079.5	330.26	44.21	6505.29	90.35	687.09	11795.36	1.79	-8095.38	10.32
2079-2098	**2088.5**	**630.64**	**32.12**	**6731.61**	**93.49**	**1551.46**	**14399.69**	**2.11**	**-13526.44**	**38.52**

Climate analysis methodology references

Hobday, A. J., Alexander, L. V., Perkins, S. E., Smale, D. A., Straub, S. C., Oliver, E. C. J., Benthuysen, J. A., Burrows, M. T., Donat, M. G., Feng, M., Holbrook, N. J., Moore, P. J., Scannell, H. A., Sen Gupta, A., and Wernberg, T.: A hierarchical approach to defining marine heatwaves, Prog. Oceanogr., https://doi.org/10.1016/j.pocean.2015.12.014, 2016.

Murphy, J. M., Harris, G. R., Sexton, D. M. H., Kendon, E. J., Bett, P. E., Clark, R. T., Eagle, K. E., Fosser, G., Fung, F., Lowe, J. A., McDonald, R. E., McInnes, R. N., McSweeney, C. F., Mitchell, J. F. B., Rostron, J. W., Thornton, H. E., Tucker, S., and Yamazaki, K.: UKCP18 Land Projections: Science Report, Met Off. Hadley Cent., 2018.

O'Dea, E., Furner, R., Wakelin, S., Siddorn, J., While, J., Sykes, P., King, R., Holt, J., and Hewitt, H.: The CO5 configuration of the 7 km Atlantic Margin Model: large-scale biases and sensitivity to forcing, physics options and vertical resolution, Geosci. Model Dev., 10, 2947–2969, https://doi.org/https://doi.org/10.5194/gmd-10-2947-2017, 2017.

Palmer, M. D., Howard, T. P., Tinker, J., Lowe, J., Bricheno, L., Calvert, D., Edwards, T., Gregory, J. M., Harris, G., Krijnen, J., Roberts, C. D., and Wolf, J.: UKCP18 Marine Report, Met Office Hadley Centre, Exeter, UK., 133 pp., 2018.

Tinker, J.: Physical Marine Climate Projections for the North West European Shelf Seas: NWSPPE, https://doi.org/doi:10.5285/edf66239c70c426e9e9f19da1ac8ba87., 2023.

Tinker, J., Renshaw, R., Barciela, R., and Wood, R.: Regional mean time series for the Northwest European Shelf seas. In: Copernicus Marine Service Ocean State Report, Issue 3, J. Oper. Oceanogr., 12, s26–s30, https://doi.org/https://doi.org/10.1080/1755876X.2019.1633075, 2019.

Wakelin, S. L., Holt, J., Blackford, J., Allen, I., Butenschön, M., and Artioli, Y.: Modeling the carbon fluxes of the northwest European continental shelf: Validation and budgets, J. Geophys. Res. Ocean., 117, C05020, https://doi.org/DOI: 10.1029/2011JC007402, 2012.

Williams, K. D., Copsey, D., Blockley, E., Bodas-Salcedo, A., Calvert, D., Comer, R. E., Davis, P., Graham, T., Hewitt, H. T., Hill, R., Hyder, P., Ineson, S., Johns, T. C., Keen, A. B., Lee, R. W., Megann, A., Milton, S. F., Rae, J. G. L., Roberts, M. J., Scaife, A., Schiemann, R., Storkey, D., Thorpe, L., Watterson, I. G., Walters, D. N., West, A., Wood, R. A., Woollings, T., and Xavier, P. K.: The Met Office Global Coupled model 3.0 and 3.1 (GC3 & GC3.1) configurations, J. Adv. Model. Earth Syst., 10, 357–380, https://doi.org/https://doi.org/10.1002/2017MS001115, 2018.

Yamazaki, K., Sexton, D. M. H., Rostron, J. W., McSweeney, C. F., Murphy, J. M., and Harris, G. R.: A perturbed parameter ensemble of HadGEM3-GC3.05 coupled model projections: part 2: global performance and future changes, Clim. Dyn., 56, 3437–3471, https://doi.org/10.1007/s00382-020-05608-5, 2021.